

# The neurocranium of the Lower Carboniferous shark *Tristychius arcuatus* (Agassiz, 1837)

Michael I. Coates and Kristen Tietjen

Department of Organismal Biology and Anatomy, University of Chicago, 1027 E 57<sup>th</sup> St, Chicago, IL 60637, USA.  
Email: mcoates@uchicago.edu

**ABSTRACT:** *Tristychius arcuatus*, from the late Viséan of Scotland, is known from numerous ironstone nodule-encased specimens. These are reinvestigated using computerised tomography (CT) scanning and 3-D digital reconstruction methods. CT scans of the neurocranium (braincase) corroborate many features of the existing reconstruction, but also reveal new details of the gross proportions, the external morphology and, for the first time, features of the internal morphology, including the otic skeletal labyrinth. The unusual position of the articulation for the palatoquadrate on the ventral surface of the postorbital process is confirmed, but the area for the hyoid articulation is relocated posteriorly and the configuration of nerve foramina within the orbit is changed. A preliminary phylogenetic hypothesis is offered, suggesting a place for *Tristychius* within a sequence of early branching events in the elasmobranch lineage. In this, *Tristychius* is not resolved as a hybodontid, but is instead a stem elasmobranch possibly related to genera such as *Acronemus*, and exemplifying anatomical conditions close to the base of the Euselachii. As such, the neurocranium of *Tristychius* offers important insight into a defining feature of these early members of the anatomically advanced elasmobranchs: the origin of specialised phonoreception.



**KEY WORDS:** Chondrichthyes, Elasmobranchii, hearing, Palaeozoic, phylogeny.

*Tristychius arcuatus* (Agassiz 1837) is a medium-sized shark known from skeletal remains that are mostly preserved in ironstone nodules of the Lower Carboniferous Scottish Upper and Lower Oil Shale Groups. Our current understanding of this fish is built largely on Stan Wood's collections of new specimens, assembled in the early 1970s (Wood 1975). These fossils provided most of the material that John Dick (1978) used for his monographic description, from which *Tristychius* emerged as one of the most completely known chondrichthyans from the entire Palaeozoic. It should be acknowledged from the outset that *Tristychius* is one of the few early chondrichthyans for which the cranial and postcranial skeleton has been described from multiple specimens. However, this motherlode of data has notably failed to deliver corresponding phylogenetic clarity. For the past couple of decades, *Tristychius* has loitered near to the base of the chondrichthyan crown as a 'problematic' taxon (Maisey 2011), because its unusual morphology fails to align easily with other grades or clades of Palaeozoic sharks. Although Dick's (1978) reconstruction was included in Zangerl's (1981) Handbook of Paleoichthyology 'Chondrichthyes I', Janvier's (1996) 'Early Vertebrates' provides only a passing reference to the genus. Thus far, published adjustments to Dick's benchmark description have been minor, limited to notes on the pectoral fin obtained from slightly younger material from the Manse Burn Formation of Bearsden (Coates & Gess 2007). The aim of the present work is to re-describe the neurocranium in the light of new results obtained from computed tomographic (CT) survey of several *Tristychius* specimens. Some, but not all, of these were included in Dick's (1978) monograph, and all except one resulted from Stan Wood's dedicated field work, whether on the shore of Granton Harbour, Edinburgh, or checking nodule-bearing horizons exposed in nearby road works.

Neurocrania are rich sources of morphological data, and the material presented here both complements and makes extensive

use of detailed CT-based descriptions of *Cladodoides* (Maisey 2005), "*Cobelodus*" (Maisey 2007), *Dwykasselachus* (Coates *et al.* 2017), *Tribodus* (Lane 2010), silyrhinchid iniopterygians (Pradel 2010), *Kawichthyes* (Pradel *et al.* 2011) and, of particular relevance to the present work, *Acronemus* (Maisey 2011; see also Rieppel 1982). Notable pre-CT descriptions of fossil chondrichthyan braincases include those of *Orthacanthus* and *Tamiobatis* (Schaeffer 1981), *Egertonodus* (Maisey 1983; revised and augmented in Lane 2010), *Akmonistion* (Coates & Sequeira 1998) and *Pucapampella* (Maisey 2001a). Notably, all of these publications post-date Dick's (1978) *Tristychius* monograph.

*Tristychius* has been long been presented as a likely early hybodont (Dick 1978; Dick & Maisey 1980; Coates & Gess 2007; Maisey 2011), initially identified as such on the basis of fin spine details. However, Maisey's (1987) emended diagnosis of the Hybodontidae established a more restrictive definition, including fin spine characteristics that *Tristychius* unambiguously lacks. The phylogenetic position of *Tristychius* thus became less certain, alongside its value as a plausible exemplar of early euselachian (*sensu* Maisey 2011) conditions. Coates & Gess (2007), Lane (2010) and Pradel *et al.* (2011) each provided more-or-less consistent discussions of the likely affinities of *Tristychius*, in which its cranial morphology figured more prominently than fin spine characteristics. These studies identified *Tristychius* as an early branch from the base of the hybodont lineage. However, against this background, Davis *et al.* (2012), Dupret *et al.* (2014) and Long *et al.* (2015) delivered a contrasting result in which *Tristychius* was excluded from the crown because of its braincase plesiomorphies.

Until now, no new data have been available to test the accuracy of the existing reconstruction and these conflicting phylogenetic hypotheses. It should be noted that none of the neurocrania described in the present work is especially well preserved relative to almost intact and uncrushed specimens such as *Cladodoides* (Maisey 2005). Nevertheless, the combined

results from scanned examples when added to Dick's (1978) restoration (Fig. 1) present an informatively detailed record of the anatomy. Perhaps most significantly, the CT survey revealed the 'hidden' side of specimen NMS 1972.27.481D (Fig. 2), which is now known to contain the only laterally compressed neurocranium of *Tristychius* discovered thus far. This specimen, more than any other, transformed the shape of the braincase restoration, and provides an improved estimate of its dorso-ventral height in life. The general proportions are similar to those estimated by Dick (1978, text-fig. 9), reproduced here in Figure 1. But, in the new restoration (Fig. 3) details of the orbit and postorbital process are clearer, the attachment and articulation areas for parts of the mandibular and hyoid arches are revealed in new detail, some features are moved to new locations and several endocranial features are exposed for the first time.

Here, close comparisons are drawn with hybodontid (Maisey 1983; Lane 2010) as well as non-hybodontid braincases (Schaeffer 1981; Maisey 2005). Particular comparisons are also made with the incompletely preserved braincase of the Middle Triassic *Acronemus* (Maisey 2011), another chondrichthyan revealed in new detail by means of CT scanning but placed, thus far, like *Tristychius* with uncertainty close to the hybodontiforms and early members of the neoselachian clade.

## 1. Materials

### 1.1. Image preparation

Scans were completed by the high-resolution X-ray computed tomography facility at the University of Texas at Austin (UTCT; www.digimorph.org). Anatomical reconstructions were completed using Mimics v. 17 (biomedical.materialise.com/mimics; Materialise, Leuven, Belgium) for the three-dimensional modelling, including segmentation, three-dimensional object rendering and STL polygon creation. 3D Studio Max (Autodesk.com/products/3ds-max; Autodesk, San Rafael, USA) was used for further editing of the STLs (color, texture, lighting) and mirroring for the final restoration.

### 1.2. Abbreviations

Explanations of anatomical abbreviations are provided in figure captions. Terminology follows Dick (1978), Maisey (1983, 2005) and Lane (2010).

**Institutional abbreviation.** NMS, National Museum of Scotland, Edinburgh, Scotland.

### 1.3. Specimens and geological context

All seven specimens used in this study were found on Wardie Beach, Edinburgh (Dineley & Metcalf 1999). Each braincase (and other associated skeletal remains) is preserved in a siderite nodule, and the fossil cartilage is often laced with pyrite. Dick (1998) described these nodules as extremely refractory, and noted the poor preservation of scales, teeth and spines. Calcified cartilage, however, has survived somewhat better, but it is often difficult to recognise on fractured surfaces of broken concretions, and difficult to prepare from the surrounding matrix. Unlike the actinopterygians from Wardie, which are usually flattened, the shark fossils have been described as 'almost uncrushed' (Dineley & Metcalf 1999). In fact, as is apparent from the present description, all specimens are crushed to some degree, and most have lost an estimated 70 % of their height or width along the axis of compaction.

Fossil fishes have been collected from Wardie since the 1830s. In addition to Dick's (1978, 1981, 1998; Dick & Maisey

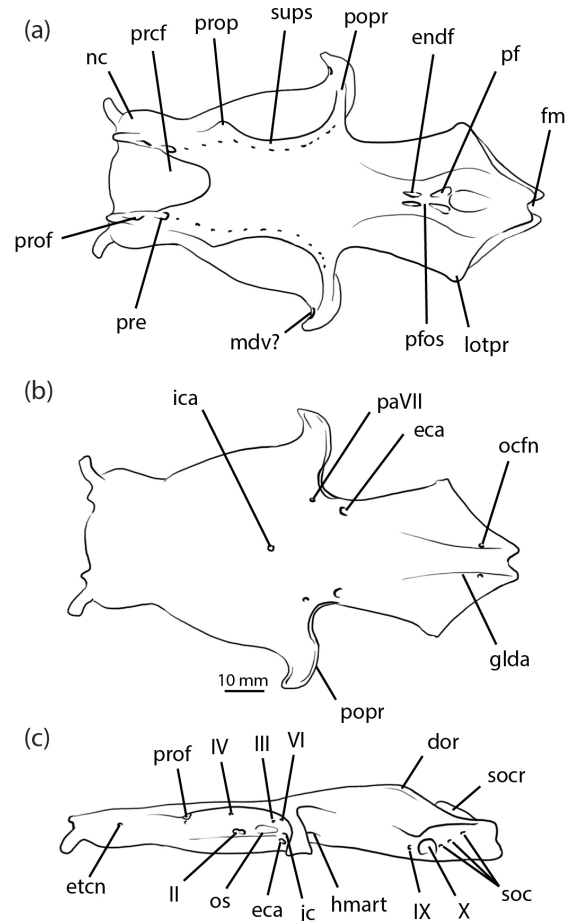


**Figure 1** *Tristychius arcuatus*, neurocranium restoration from Dick 1978: (a) dorsal view; (b) ventral view; (c) lateral view. Abbreviations: dor = dorsal otic ridge; eca = external carotid artery foramen; endf = endolymphatic foramen; etcn = ethmoid canal; fm = foramen magnum; glda = groove for lateral dorsal aorta (common carotid artery); hmart = hyomandibula articulation area; ica = internal carotid artery foramen; jc = jugular canal; lotpr = lateral otic process; mdv? = mandibular vein foramen; nc = nasal capsule; ocfn = occipital artery foramen; os = optic stalk attachment; paVII = palatine branch of facial nerve foramen; pf = perilymphatic fenestra; pfos = parietal fossa; popr = postorbital process; prcf = precerebral fontanelle; pre = preorbital canal; prof = profundus nerve foramen; prop = preorbital process; soc = spino-occipital nerve foramina; socr = supraoccipital crest; sups = supraorbital shelf; II = optic nerve foramen; III = oculo-motor nerve foramen; IV = trochlear nerve foramen; VI = abducens nerve foramen; IX = glossopharyngeal nerve foramen; X = vagus nerve foramen.

1980) descriptions of the fossil sharks, classic reviews of the fishes include those by Traquair (1903) and Wood (1975). Descriptions of the site geology have been presented by Peach *et al.* (1910), Waterston (1962), Mitchell & Mykura (1962), Wood (1975) and Clarkson (1986). The shark assemblage from which the *Tristychius* material derives, named the *Diplodoseleche* fauna (Dick 1981), is characteristic of the nodules of the Oil Shale Group, the Burdiehouse Limestone, and the roof shales of the Lower Limestone coal seams, the Limestone Coal and the Upper Limestone groups (Dineley & Metcalf 1999). This places the age somewhere between the uppermost Viséan and lowermost Serpukhovian (see also Dick 1998).

Six of the specimens were collected by Stan Wood in the early 1970s, and the seventh (NMS G. 2015.30.1A, B) (Fig. 4) was discovered a century earlier by another remarkable and largely self-taught palaeontologist, Charles Peach (Taylor &

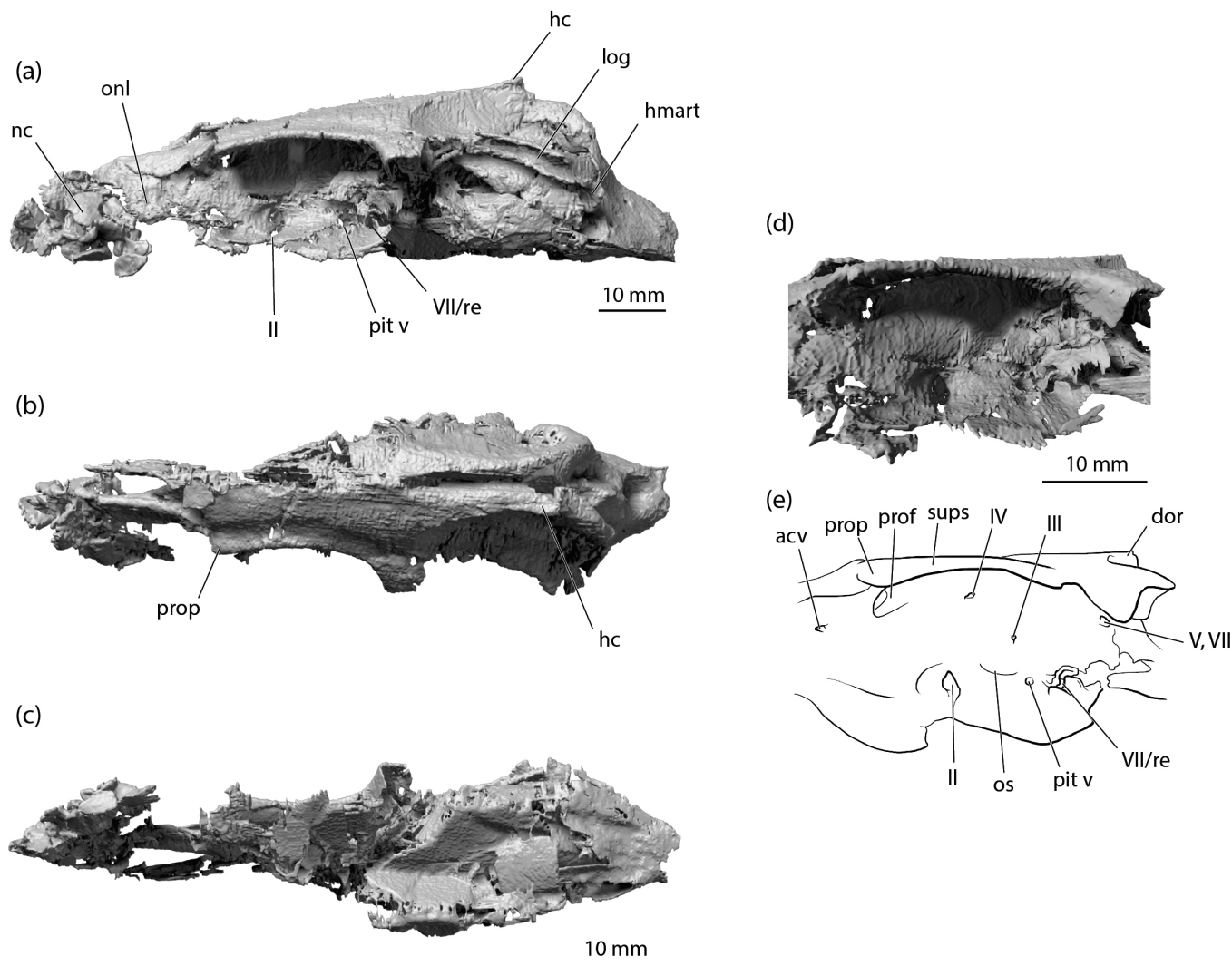


**Figure 2** *Tristychius arcuatus*, NMS 1972.27.481D, rendering of CT scan showing complete, laterally compressed neurocranium: (a) left lateral view; (b) dorsal view; (c) ventral view; (d) detail of left orbit; (e) line drawing of rendering shown in (d). Abbreviations: acv = anterior cerebral vein foramen; dor = dorsal otic ridge; hc = horizontal crest; hmart = hyomandibula articulation area; log = lateral otic groove; nc = nasal capsule; onl = orbitonasal lamina; os = optic stalk base; pit v = pituitary vein foramen; prof = profundus nerve foramen; prop = preorbital process; re = insertion for external rectus muscle; sups = supraorbital shelf; II = optic nerve foramen; III = oculomotor nerve foramen; IV = trochlear nerve foramen; V, VII = trigemino-facial foramen; VII = foramen for anterior branch of facial nerve.

Anderson 2015). All of these specimens are deposited in the collections of the National Museums of Scotland, Edinburgh. Besides *Tristychius*, at least three other chondrichthyan genera are known from the *Diplodoselache* fauna: the eponymous *Diplodoselache* (Dick 1981); *Onychoselache* (Dick 1978; Dick & Maisey 1980; Coates & Gess 2007); and *Sphenacanthus* (Dick 1998).

## 2. Systematic palaeontology

Class Chondrichthyes (Huxley 1880)  
Cohort Euselachii (Hay 1902; *sensu* Maisey 2011)  
*Incertae sedis* Genus *Tristychius* (Agassiz 1837)

**Emended diagnosis.** Euselachian shark distinguishable from other euselachian genera by the structure of the postorbital attachment of the upper jaw, in that the otic process of the palatoquadrate articulates with single, broad ridge and groove on the ventral surface of the postorbital process. The sub-orbital shelf is exceptionally wide, and the narrower supraorbital

shelf terminates anteriorly with a prominent preorbital process. Dorsal otic ridges flanking the parietal fossa each bear a narrow horizontal crest; a short, acute, supraoccipital crest is present. Finspines with many (11 to 15) costae dorsally, decreasing in number ventrally towards the spine's insertion, to between three and eight costae which lie near its anterior border; posterior surface of finspine flat or concave.

Species *Tristychius arcuatus* (Agassiz 1837)

**Diagnosis.** As for genus

**Referred specimens.** See Dick (1978) for list of *Tristychius arcuatus* specimens; an additional specimen is listed in Coates & Gess (2007).

NMS 1972.27.461A & B (Dick 1978, text-fig. 11): head of fish preserved in the round, of negligible value for CT scan because little of the original skeletal structure is preserved, Wardie sea-shore 'locality B'; collected by S. P. Wood.

NMS 1972.27.481D (Figs 2, 7a, 8, 9a, 11a–d); Dick 1978, text-fig. 8A): laterally compressed braincase, as such thus far



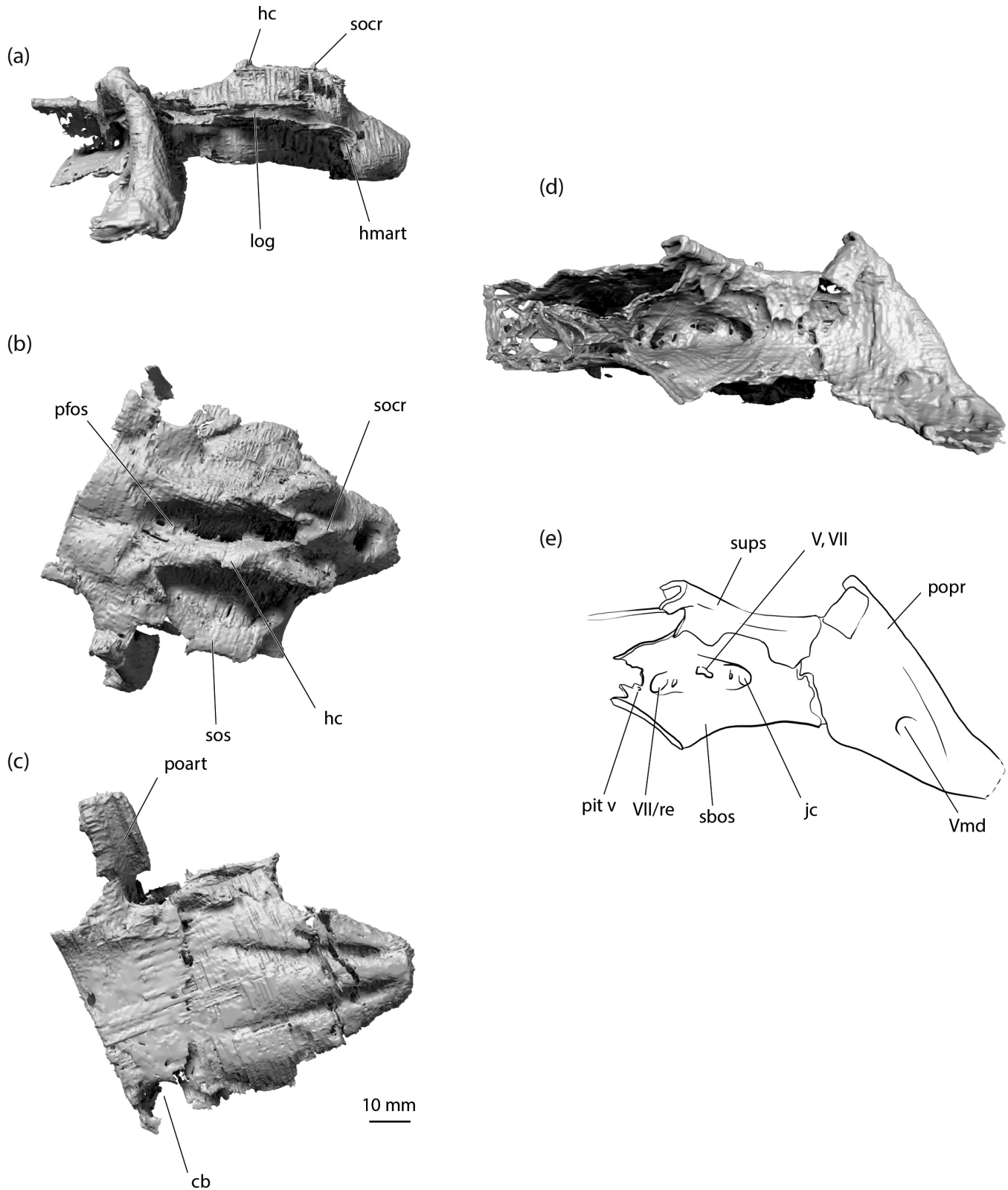


**Figure 4** *Tristychius arcuatus*, NMS G. 2015.30.1A & B, Peach specimen, dorsoventrally compressed otic and occipital region: (a) left lateral view; (b) dorsal view; (c) ventral view; (d) anterolateral view of orbit posterior and trigeminofacial recess; (e) line drawing of rendering in (d). Abbreviations: cb = C-bout; hc = horizontal crest; hmart = hyomandibula articulation area; jc = jugular canal; log = lateral otic groove; pfos = parietal fossa; pit v = pituitary vein canal; poart = postorbital articulation; popr = postorbital process; re = insertion for external rectus muscle; sbos = suborbital shelf; socr = supraoccipital crest; sos = supraotic shelf; sups = supra-orbital shelf; Vmd = mandibular branch of trigeminal nerve foramen; V, VII = trigeminofacial foramen; VII = foramen for anterior branch of facial nerve.

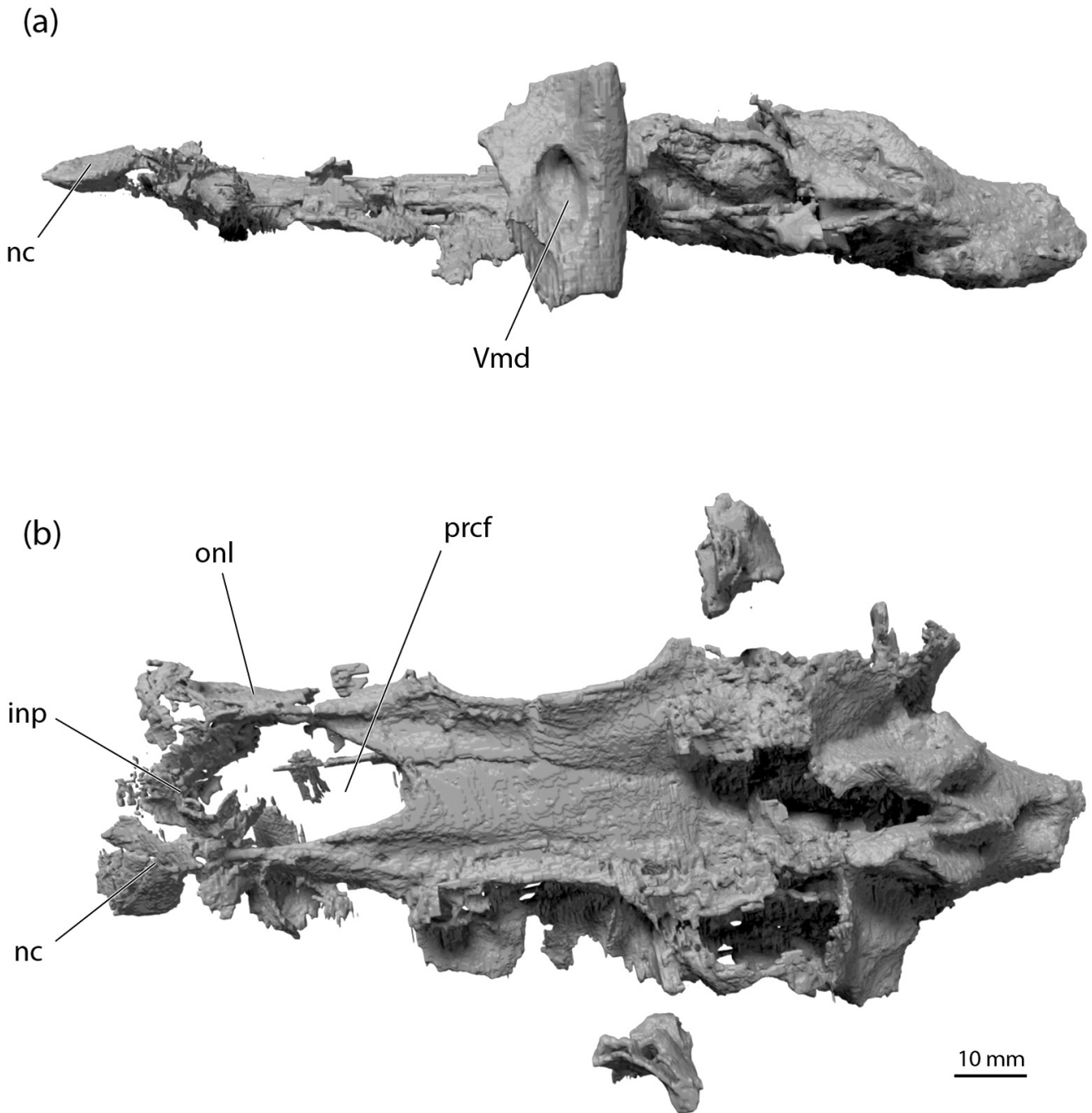


**Figure 5** *Tristychius arcuatus*, NMS 1974.23.6, rendering of CT data showing dorsoventrally compressed neurocranium: (a) left lateral view; (b) dorsal view. Abbreviations: inp = internasal plate; nc = nasal capsule; onl = orbitonasal lamina; prcf = precerebral fontanelle; Vmd = mandibular branch of trigeminal nerve foramen.

appears that the ‘accessory cartilage’ noted by Dick is no more than a fragment of the posterolateral wall of a capsule. Thus, the orbits and nasal capsules are separated by a substantial length of preorbital or postnasal wall, resembling the orbitonasal lamina of chimaeroids (De Beer 1937) or the extended pre-orbital region in *Heterodontus* (Daniel 1922). The most completely preserved nasal capsule is from the left side of NMS 1972.27.481D (Fig. 2a) and although laterally crushed, it indicates that the nasal openings were directed anterolaterally. In *Tristychius* the nasal capsules are separated ventrally by an internasal plate, and dorsally by a broad precerebral fontanelle (Fig. 5b, NMS 1974.23.6). There is no clear evidence of a rostral bar on the ventral surface of the internasal plate, as found in hybodontids (Maisey 1983), but the preservation of this area in *Tristychius* is poor.

The precerebral fontanelle is well formed, large, and extends back to the anterior margin of the supraorbital shelves. The general proportions and relation to flanking grooves and foramina for the lateral line nerve component of the superficial ophthalmic trunk closely match Dick’s (1978) interpretation.

### 3.2. Orbit

Specimens preserving the most complete and most informative sections of the orbit are NMS 1972.27.481D and NMS G. 2015.30.1. The orbit is floored with a broad suborbital shelf and roofed by a narrower supraorbital shelf, in agreement with Dick’s (1978) description. In CT scans, the suborbital shelf tends to be poorly resolved, because this wide cartilage sheet usually forms a breakage plane between part and counterpart of a nodule, and calcified material flakes away from the

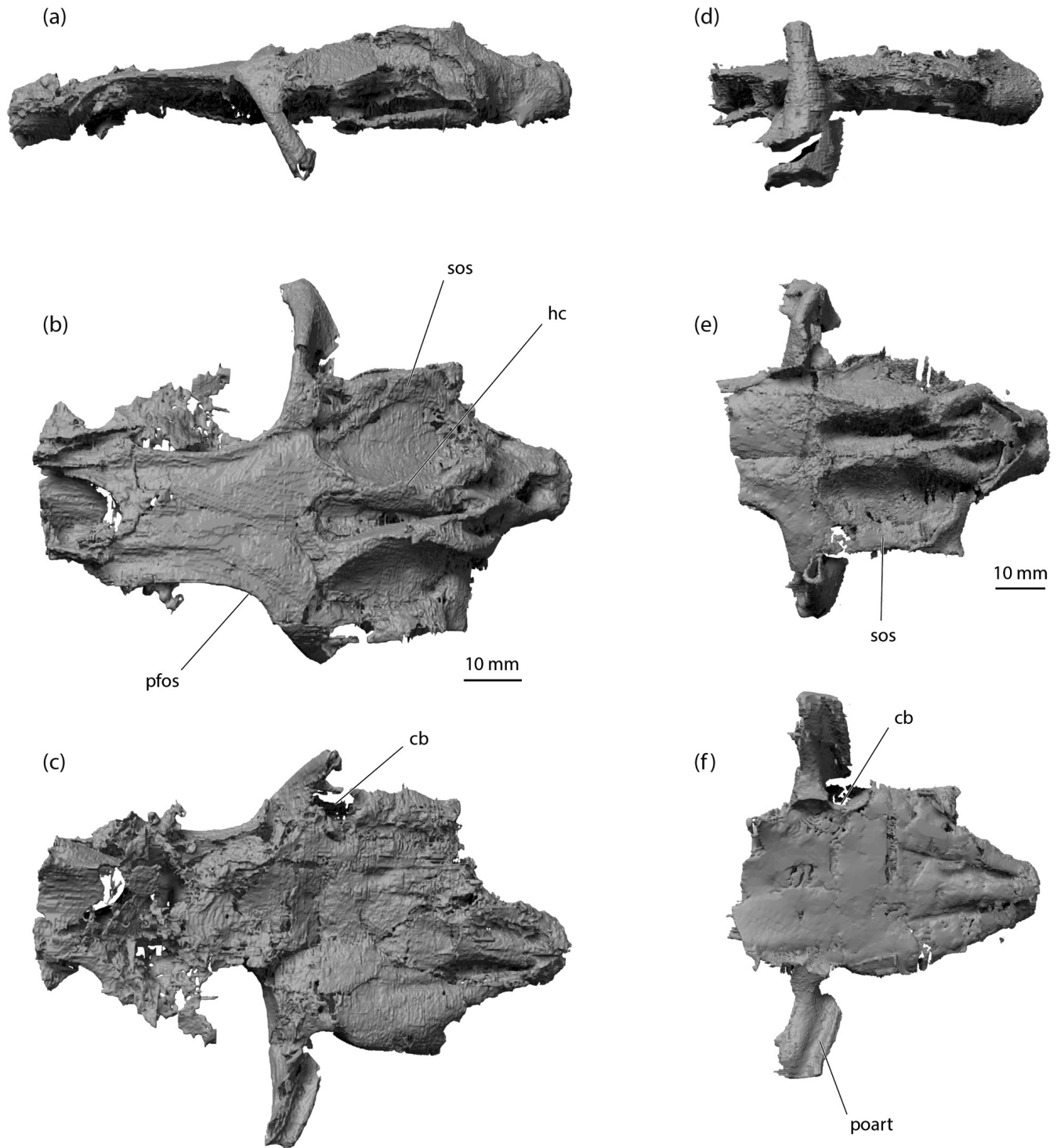


**Figure 6** *Tristychius arcuatus*. (a–c) NMS 1974.23.30A & B, rendering of CT data showing complete, dorsoventrally compressed neurocranium: (a) left lateral view; (b) dorsal view; (c) ventral view. (d–f) NMS 1974.51.2A & B, rendering of CT data showing dorsoventrally compressed otic and occipital region: (d) left lateral view; (e) dorsal view; (f) ventral view. Abbreviations: cb = C-bout; hc = horizontal crest; pfos = parietal fossa; poart = postorbital articulation; sos = supraotic shelf.

exposed surfaces. Importantly, the suborbital shelf includes no evidence of palatobasal flange-like articulation process such as those present in symmoriids (notably apparent in *Ozarcus* (Pradel *et al.* 2014).

The supraorbital shelf has a gently concave lateral edge that extends posterolaterally to blend smoothly into the descending postorbital processes. A shallow groove on the dorsal surface parallels the lateral margin, and within this lies the small foramina for twigs of the superficial ophthalmic trunk, as noted by Dick (1978). Similar features are present in *Egertonodus*

(Maisey 1983; Lane 2010). Anteriorly, the supraorbital shelf terminates as a small but robust preorbital process, the dorsal position of which distinguishes it clearly from the ectethmoid process of *Egertonodus* (Maisey 1983).

The orbit wall is most complete in NMS 1972.27.481D (Fig. 2), but this is broken around the perimeter because of lateral compression. Consequently, a deep recess leading to a profundus foramen/preorbital canal is preserved, but this is situated within a damaged (compression fractured) area of cartilage. At the anterior margin of the orbit, where it blends

smoothly with the lateral face of the orbitonasal lamina, a small foramen resembling the anterior cerebral vein foramen in *Cladodoides* is situated anteroventrally to the preorbital process. The optic nerve foramen lies within a recess at the centre and base of the orbit wall, where it meets the proximal margin of the suborbital shelf. The trochlear nerve foramen (in NMS 1972.27.481D) is well preserved, close to the orbit roof, dorsal but slightly posterior to the anteroposterior level of the optic nerve foramen (Fig. 2d, e). This conflicts with Dick's restoration, which places the trochlear foramen anterior to the optic nerve foramen, but is more consistent with his illustration of NMS 1973.24.41 (Dick 1978, text-fig. 4) which shows the trochlear and optic foramina at the same level.

The oculomotor nerve foramen is preserved in NMS 1972.27.481, but concealed in lateral view by a displaced cartilage plate. There is no outgrowth in the orbit wall indicating the presence or base of an optic pedicel. However, a small depression and horizontal groove posterior to the optic nerve foramen resembles Dick's estimate of an optic stalk base, and the feature that Schaeffer (1981) identified as the optic stalk depression in *Tamiobatis*.

The posterior portion of the orbit resembles the arrangement of foramina and canals in *Tamiobatis* (Schaeffer 1981, fig. 7) or *Cladodoides* (Maisey 2005, fig. 17B) rather more than conditions in *Egertonodus* (Maisey 1983; Lane 2010). A broad trigeminofacial recess is continuous with the anterior opening of the jugular canal. This is preserved best in the dorsoventrally compressed specimen NMS G. 2015.30.1 (Fig. 4d, e). The medial wall of the recess includes a broad, laterally directed foramen for the trigeminal nerve and anterodorsal lateral line nerves. Anteroventral to this, preserved in NMS 1972.27.481D (Fig. 2a, d, e) there is a large, flared opening, which is also preserved, although less offset ventrally in NMS G. 2015.30.1 (Fig. 4d, e). This distinctive feature might represent the exit of the anterior branch of the facial nerve. However, this places the nerve foramen in a more dorsal location than the far-better-preserved example in *Cladodoides* (Maisey 2005). Alternatively, this recess could mark the insertion of the external rectus muscle, thereby unexpectedly resembling the paired posterior myodome of early actinopterygians (Gardiner 1984). Once again, *Cladodoides* provides a plausible template for this interpretation (Maisey 2005, fig. 16A). Other foramina and structures from this region in *Tristychius* are poorly preserved, because orbit wall is variously crushed and shattered, but the pituitary vein canal appears to be preserved, located just anterior to the larger recess for nerve or muscle, in both NMS 1972.27.481D and NMS G. 2015.30.

### 3.3. Postorbital process

The postorbital process and wall is most completely preserved in specimens NMS 1974.23.30, NMS 1974.51.2. and NMS G. 2015.30.1. Like those of *Acronemus* (Maisey 2011), the postorbital processes of *Tristychius* have been less affected by dorsoventral compaction than other neurocranial regions (*cf.* Figs 4a, 5a, 6d). The general form of the process, anteroposteriorly narrow, proximally, and downturned laterally and more substantially structured distally, resembles those depicted and restored by Dick (1978, text-fig. 6). Each is thoroughly mineralised, probably to act as a buttress against forces conveyed from the jaws and jaw musculature. The postorbital wall (the anterior face of the process) is extensive and perforated by the jugular vein in the ventromedial corner. In lateral view, the process is narrow dorsally, but flares and thickens ventrally to form an anteroposteriorly broad 'foot'. In this regard it differs from the parallel sided postorbital process of *Acronemus* (Rieppel 1982, text-fig. 1), but like *Acronemus* there is an anhe-  
dral angle between the base of the process and the basicranium

(Figs 3d, 4d). Therefore, *contra* Coates & Gess (2007), the *Tristychius* postorbital process can, in fact, be characterised as extending a short distance below the rest of the basicranium (see also note in Maisey 2011). The articular area is confined to the ventral surface, and therefore occupies that part of the postorbital process that is inferred as derived from the embryonic lateral commissure (de Beer 1937). The location of this surface is in marked contrast to the more general condition of early chondrichthyans, in which a groove extends dorsoventrally across the posterior of the postorbital process, as shown especially clearly in *Dwykasselachus* (Coates *et al.* 2017). In *Tristychius*, the articulation surface consists of a single, slightly anterolaterally directed, gently curved broad ridge and groove (Figs 4c, 6f). Unlike *Acronemus*, no part of the articular area extends onto the posterior surface. The simplicity of the articular surface shape suggests that the palatoquadrates were capable of some postero-medial to antero-lateral movement.

In agreement with Dick (1978), aside from the jugular canal, the only foramen present in the anterior surface of the process is positioned ventrally and distally (Figs 4e, 5a). This is the anterior opening of a canal resembling a similarly located channel through the postorbital process of *Cladodoides*, interpreted as carrying the mandibular branch of the trigeminal nerve (Maisey 2005). The proximal opening of the canal is positioned opposite the likely foramen of the exit of the trigeminal nerve in the anteriormost part of the otic wall.

### 3.4. Basicranium

The basicranial region is most completely preserved in specimens NMS 1974.23.30, NMS 1974.51.2, and NMS G. 2015.30.1. These examples add little to Dick's (1978) description, but it is now apparent that the grooves for the lateral dorsal aortae are arranged very like those of *Acronemus* (Maisey 2011, text-fig. 2A). In ventral view, the posterior profile of the junction between the otic wall and the base of the postorbital process is markedly concave, resembling the C-bout of a violin waist (Figs 4c, 6c, f). This feature, once again, is shared with *Acronemus*, and might signal the location of the spiracular pouch, although chondrichthyan neurocrania are not known to bear a clear morphological marker of pouch location. The floor of the otic region is broad, and although preservation is of insufficient quality to show separate contributory cartilage layers, it is very likely formed by a hypotic lamina. The occipital region projects posteriorly beyond the level of the otic capsules, but, unlike Dick's (1978) restoration of *Tristychius* (Fig. 1) and unlike *Acronemus*, the occipital cotylus is not recessed deeply. Furthermore, in lateral view the occipital cotylus is offset ventrally relative to the rest of the basicranial floor, resembling hybodonts such as *Tribodus* and *Egertonodus* (Lane 2010).

### 3.5. Otic region

The otic region is well preserved in NMS 1974.23.30, NMS 1974.51.2, and NMS G. 2015.30.1. As described by Dick (1978), a well-formed ridge overlies anterior and posterior semicircular canals on each side of the dorsal midline, and these ridges converge to flank an elongate parietal fossa with a chondrified floor (Dick's 'median supraotic fossa'). Unexpectedly, these ridges exhibit horizontal crests (Figs 2b, 4a, b, 6b), like those of *Orthacanthus* and especially *Tamiobatis* (Schaeffer 1981), rendered indistinctly in *Cladodoides* (Maisey 2005), and identified in an apparently reduced form in *Akmonistion* (Coates & Sequeira 1998). In *Tristychius*, the posterior extremity of this horizontal crest appears to overlie the posterior boundary of the anterior semicircular canal. The posterior portion of the ridge is smooth, rounded and, in lateral view, conforms closely to the arc of the enclosed canal (*cf.* Dick, 1978, text-fig. 8A).



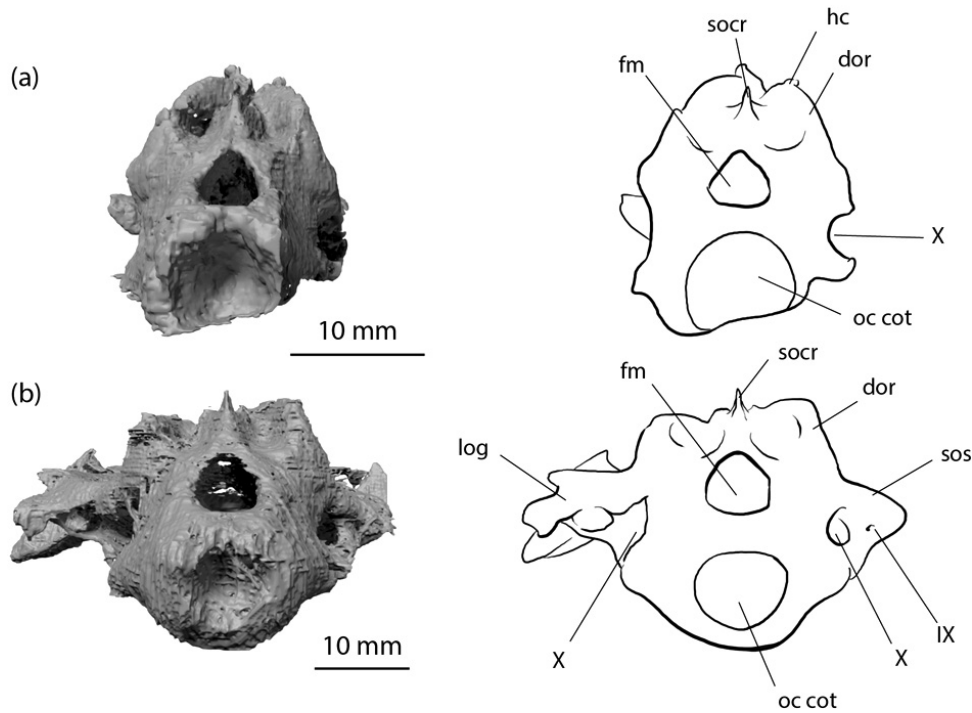


**Figure 7** *Tristychius arcuatus*, occipital views of (a) NMS 1972.27.481D, (b) NMS G. 2015.30.1A & B; each with line drawings. Abbreviations: dor = dorsal ridge; fm = foramen magnum; hc = horizontal crest; log = lateral otic groove; oc cot = occipital cotylus; socr = supraoccipital crest; sos = supraotic shelf; IX = glossopharyngeal foramen; X = vagus foramen.

The parietal fossa lacks a distinct anterior boundary, unlike the fossa in *Egertonodus* and *Tribodus*, and the floor is continuous with the cranial roof between the orbits (Figs 4b, 6b). As identified by Dick (1978), separate endolymphatic openings and perilymphatic fenestrae perforate the fossa walls. The posterior of the fossa rises to form the anterior face of a subtriangular platform from which extends posteriorly and dorsally a short, acute supraoccipital crest, best preserved in NMS G. 2015.30.1 (Figs 4b, 7b). The posterior apex of the crest (and platform) extends posteroventrally to the roof of the foramen magnum. Ridges overlying left and right posterior semicircular canals converge anteriorly to meet the platform so that this complex forms a ‘W’ shape in dorsal view, with a ‘V’-shaped fossa on either side of the base of the occipital crest (Figs 4b, 5b, 6b, e). In this respect, *Tristychius* exhibits a mixture of conditions in *Egertonodus* (Maisey 1983, fig. 8; Lane 2010, fig. 29A) and *Orthacanthus* (Schaeffer 1981, figs 5, 6). Notably, like *Acronemus*, but unlike the xenacanth, *Tamiobatis* and *Cladodoides*, the posterior semicircular canal is oriented posterolaterally to flank the dorsal part of the occipital unit. The canal is not enclosed by or directed towards a lateral otic process (cf. Maisey 2011).

Behind the postorbital process, the otic roof forms a very broad supraotic shelf, once more resembling conditions in *Acronemus* (Maisey 2011). This shelf is thinly calcified but complete, unlike the shelf in *Tamiobatis vetustus* (Schaeffer 1981). The lateral extremity of the shelf projects as a slender horizontal flange beyond the main body of the lateral otic ridge. The anteriormost part of the flange terminates at a C-bout, more-or-less matching the corresponding profile on the basicranial surface. Behind the C-bout, the extreme lateral rims of these shelves or flanges are nearly parallel on left and right sides. Thus, in dorsal and ventral views, the otic region (posterior to the postorbital processes and anterior to occiput) is nearly rectangular (unlike the kite-shaped restoration in

Dick 1978). This flange terminates posteriorly, anterior to the posterolateral extremity of a second, lower otic flange (or shelf) (Figs 4b, 6b, e). Between these otic outgrowths, a lateral otic groove resembles the jugular groove of *Pucapampella* (Maisey 2001). However, in *Tristychius* this groove (Figs 2a, 4a) is situated dorsal to the jugular canal exit. Posteriorly, the shelf forming the groove floor flares laterally and curves ventrally to scroll over the hyomandibula attachment area (Figs 2a, 4a). Dick (1978) identified this region as the ‘otic process’, and it lies directly anterior and dorsal to the separate foramina for the glossopharyngeal and vagus nerves (cf. Dick 1978). Maisey (2011) identified a corresponding posterolateral extremity in *Acronemus* as the ‘periotic process’, but this term is not used here in order to avoid confusion with the unrelated periotic process of “*Cobelodus*” (Maisey 2007). Notably, in *Tristychius* there is no lateral otic process in the sense of the term as used by Schaeffer (1981) for *Orthacanthus* and *Tamiobatis*.

### 3.6. Occipital region

The occipital region is reasonably well preserved in all specimens in the present study, and the proportions are much as described by Dick (1978). In dorsal and ventral views, although the otic regions are exceptionally similar in *Tristychius* and *Acronemus*, the occiput projects posteriorly to a far greater degree in *Tristychius* than in *Acronemus*. In lateral view, the occipital wall is punctured by a series of three foramina for spinooccipital nerves. In posterior view the large foramen for the vagus nerve is clearly visible, medial to the smaller glossopharyngeal nerve foramen. In occipital view (Fig. 7), the cotylus is slightly wider than the foramen magnum. Dorsally, the occipital crest is flanked by fossae which are themselves limited laterally by the posterior of the dorsal otic ridge. A similar arrangement is manifest in *Egertonodus* (Maisey 1983, fig. 9E) and *Tribodus* (Lane 2010, fig. 12B). Likewise, the occipital view shows the

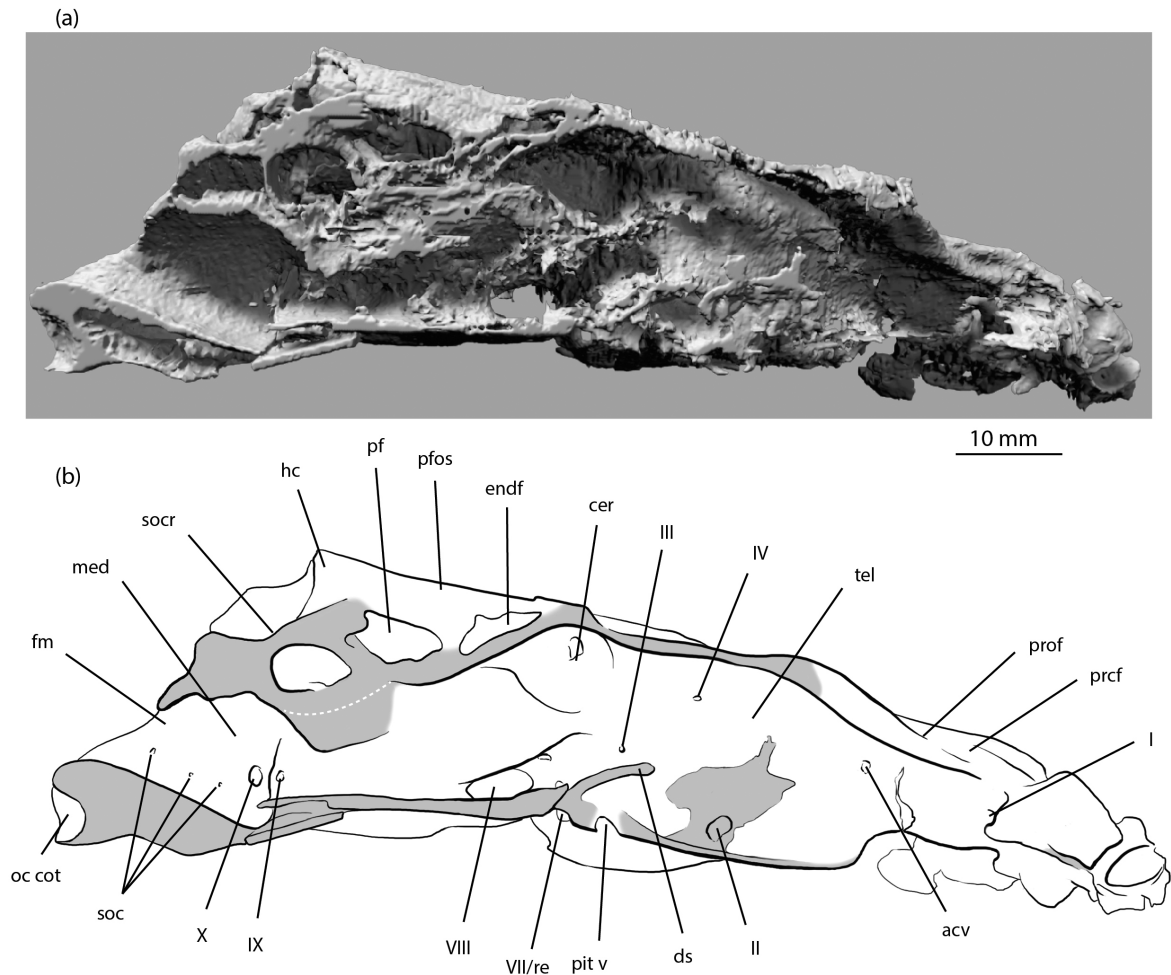


**Figure 8** *Tristychius arcuatus*, NMS 1972.27.481D, medial view of left side in sagittal section: (a) rendering from CT data; (b) line drawing showing major features of the endocranium, including the fractured sections of the floor. Grey shading signifies sectioned cartilage, including displaced laminae obscuring anatomical landmarks such as the optic nerve foramen. Abbreviations: acv = anterior cerebral vein foramen; cer = cerebellar region; ds = dorsum sellae; endf = endolymphatic foramen; fm = foramen magnum; hc = horizontal crest; med = medullary region; oc cot = occipital cotylus; pf = perilymphatic fenestra; pfos = parietal fossa; pit v = pituitary vein foramen; prcf = precerebral fontanelle; prof = profundus nerve foramen; re = insertion for external rectus muscle; soc = spino-occipital nerve canals; socr = supraoccipital crest; tel = telencephalon region; I = olfactory tract canal; II = optic nerve foramen; III = oculomotor foramen; IV = trochlear foramen; VII = foramen for anterior branch of facial nerve; VIII = octaval nerve foramen; IX = glossopharyngeal nerve foramen; X = vagus nerve foramen.

relation of the lateral extremities of the otic capsule and lateral otic groove to the occiput, and the similarity of this arrangement to the so-called lateral otic process of *Egertonodus* (Maisey 1983, fig. 9E) and the hyomandibular articulation in *Tribodus* (Lane 2010, fig. 12B).

### 3.7. Endocranium and endocasts

The walls of the endocranial spaces are preserved best in NMS 1972.27.481D (Fig. 8). The condition of the walls is poor and far worse than in barely distorted neurocrania such as those of *Egertonodus* (Lane 2010) or *Dwykasselachus* (Coates *et al.* 2017). Nevertheless, some general and fairly conservative observations are possible.

In medial view (sagittal section), similarities with *Egertonodus* (Lane 2010, fig. 34) are more numerous than with *Cladodoides* (Maisey 2005, fig. 7), the most significant of which is the presence of a medial capsular wall. Ventrally, this is pierced by a large opening that appears to have been for the octaval nerve. Notably, the opening is single and not divided into two, as in *Tribodus* and *Egertonodus* (Maisey 2004; Lane 2010). In NMS 1972.27.481D, this communicates between the

main cranial cavity and extracranial space instead of the expected interior of the otic capsule. This a side-effect of *post mortem* damage to the ventral part of the external, otic capsule wall.

Anterior to the otic region, the dorsum sellae is low and projects anteriorly above the basicranial fenestra for the internal carotid arteries. Although poorly shown in cross-section (Fig. 8), this forms a complete shelf spanning the endocranial cavity above the hypophyseal space. Note that the ventrally facing notch shown in Figure 8 is more likely a displaced part of the pituitary vein canal (pit v) in the concertinaed basicranium of NMS 1972.27.481D. The exit for the optic nerve is obscured by a displaced piece of cartilage. Further anteriorly, the exit for the olfactory nerve is visible. The posterior part of the endocranial, sagittal section cuts through the depressed floor of the parietal fossa, dorsal to exits of glossopharyngeal nerve and vagus nerve. This is markedly similar to conditions in *Egertonodus* (Lane 2010, fig. 34).

A virtual endocast of NMS 1972.27.481D (Fig. 9a) provides a limited (in terms of detail) but general comparison with other early chondrichthyan examples. The gross proportions most

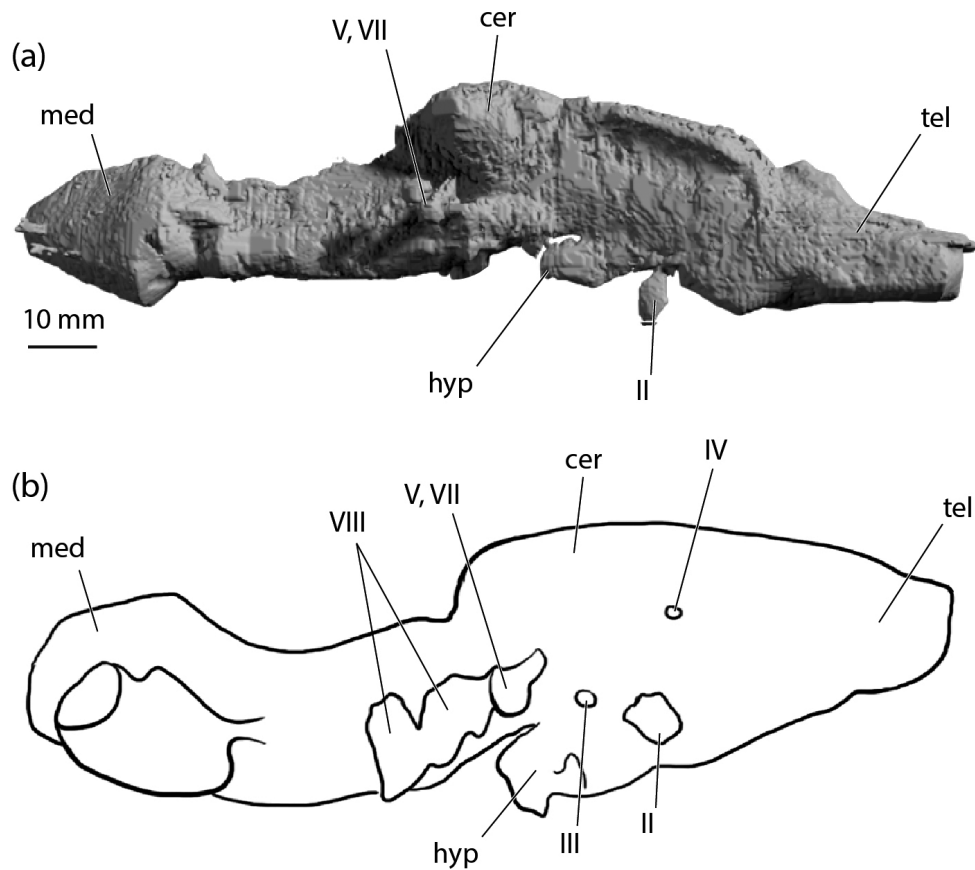


**Figure 9** Euselachian cranial cavity endocasts: (a) *Tristychius arcuatus*, NMS 1972.27.481D, endocast in right, lateral view; (b) *Egertonodus basanus*, redrawn after Lane (2010, fig. 35), reversed for ease of comparison. Abbreviations: cer = cerebellar region; hyp = hypophyseal recess; med = medullary region; tel = telencephalon region; II = optic nerve foramen; III = oculomotor foramen; IV = trochlear foramen; V, VII = trigeminofacial foramen; VIII = octaval nerve foramen.

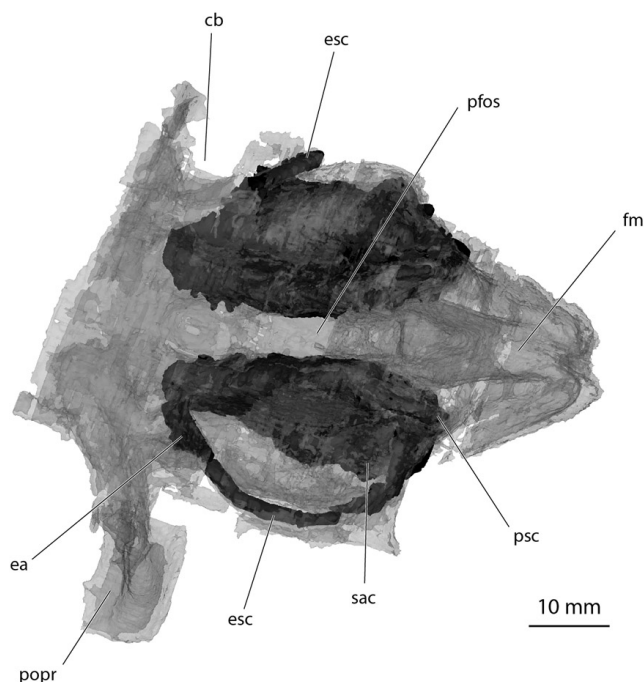


**Figure 10** *Tristychius arcuatus*, NMS G. 2015.30.1. A & B, neurocranium rendered semitransparent showing infill of otic skeletal labyrinths in dorsal view. Abbreviations: cb = C-bout; ea = external canal ampulla; esc = external canal; fm = foramen magnum; pfos = parietal fossa; popr = postorbital process; psc = posterior canal; sac = saccular chamber.

closely resemble *Egertonodus* (Lane 2010) (Fig. 9b). The space for the telencephalon blends smoothly with the cerebellar space, and the relative size of the hypophyseal chamber is smaller and shallower than those of *Cladodoides* (Maisey 2005) and “*Cobelodus*” (Maisey 2007). The infill of the optic nerve exit is displaced ventrally. This (again) is an artefact of laterally compressed preservation and concertinaed folding of the basicranial cartilage. The posterior part of the cerebellar chamber roof drops significantly as it passes beneath the floor of the parietal fossa. The most distinctive feature is the enlarged roof of the chamber of the medullary region in *Tristychius*. This is apparently absent in non-neoselachian examples, but present and strikingly similar in *Egertonodus* and *Tribodus* (Lane 2010); described by Maisey (2004) as a ‘distinct dome’ and also noted as present some extant elasmobranchs; e.g., *Notorynchus*.

Virtual endocasts of the partly crushed skeletal labyrinth have been obtained from specimen NMS G. 2015.30.1 (dorsoventrally compressed) (Figs 10, 11e–h) and NMS 1972.27.481D (laterally compressed) (Fig. 11a–d). Dick (1978) noted that parts of the labyrinth canals are also visible in NMS 1973.23.44; the same is true for NMS 1974.23.19, which includes a break through the occipital region exposing the posterior semicircular canals. Both of these specimens are dorsoventrally compressed (the usual condition of preservation).

In dorsal view, the saccular chamber of *Tristychius* is broad (Figs 10, 11e) but not wide enough to meet the external (horizontal) semicircular canal, as in *Egertonodus* and *Tribodus* (Lane 2010). Furthermore, the semitransparent CT reconstruction of NMS G. 2015.30.1 shows that the otic capsules do

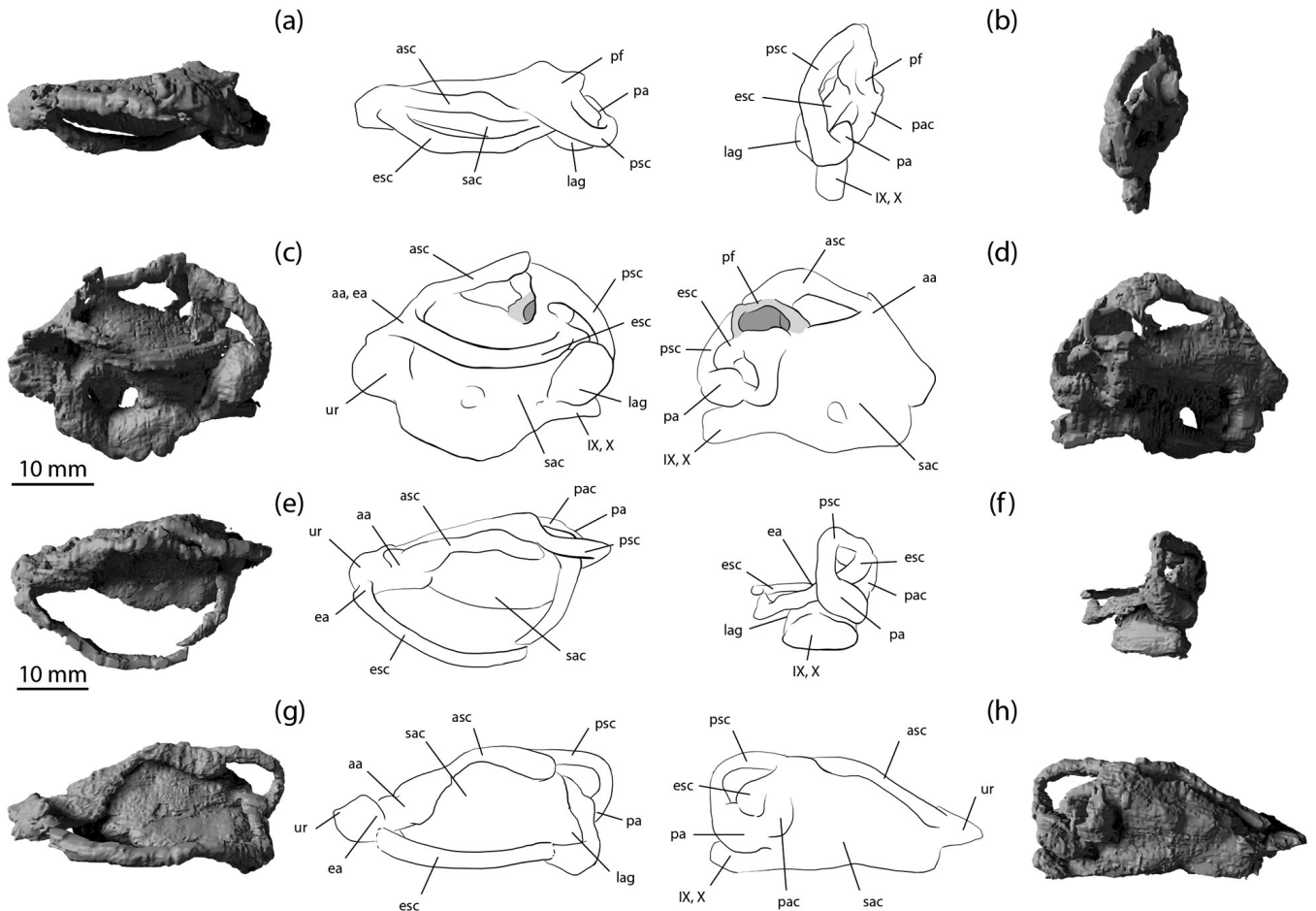


**Figure 11** *Tristychius arcuatus*, otic skeletal labyrinths shown as line drawings flanked by rendered virtual endocasts. (a–d) NMS 1972.27.481D, right otic capsule, shown in (a) dorsal, (b) posterior, (c) lateral and (d) medial view. (e–h) NMS G. 2015.30.1, left side otic capsule (reversed) shown in (e) dorsal, (f) posterior, (g) lateral and (h) medial view. Abbreviations: aa = anterior ampulla; asc = anterior canal; ea = external ampulla; esc = external canal; lag = lagenar recess; pa = posterior ampulla; pac = preampullary canal; pf = perilymphatic fenestra; psc = posterior canal; sac = saccular chamber; ur = utricular recess; IX, X = common canal for glossopharyngeal and vagus nerves.

not project anteriorly between the postorbital processes. The anteriormost extremities, the anterior ampulla and utricular recess, are located just behind the processes, as in many Palaeozoic sharks but unlike *Acronemus* (Maisey 2011).

In lateral view, the saccular chamber is partly divided from a posterior lagenar chamber (Fig. 11c). The anterior and posterior semicircular canals arise directly from the saccular chamber. Dick's (1978) interpretation of NMS 1974.23.44 implied that a sinus superior and a crus commune were present, but conditions in the differently compressed specimens studied here indicate otherwise. Notably, the left side posterior semicircular canal of NMS G. 2015.30.1 (Fig. 11h) achieves an almost complete independent arc that passes through the space occupied by a crus commune in other gnathostome clades. A dorsal perspective of the same specimen shows overlap but clear separation between anterior and posterior canals. Thus, like hybodonts and neoselachians, there is no evidence of union between anterior and posterior canals (Maisey 2001b); but unlike hybodonts, the anterior and posterior canals of *Tristychius* are not widely separated. Moreover, the radius of the arc of the anterior semicircular canal must have been significantly larger than the radius of the posterior canal. This, again, is unlike hybodonts, in which anterior and posterior canals are similarly sized. In medial view, both NMS 1972.27.481D and NMS G. 2015.30.1 show that the posterior canal includes a significant length of ascending preampullary

canal. NMS 1972.27.481D preserves this preampullary canal in clear association with the aperture of the perilymphatic fenestra. Finally, from a dorsal perspective, the oblique angle between anterior and posterior canals is unusual, as is the almost anteroposterior orientation of the anterior canal. Comparable conditions are otherwise unique to *Acronemus* (Maisey 2011, text-fig. 4)

The unusually broad sweep of the external semicircular canal is preserved best in the left side labyrinth of NMS G. 2015.30 (Fig. 10). When scaled to the same anteroposterior labyrinth length as *Egertonodus* and *Tribodus* (Lane 2010) it is possible to confirm that the external semicircular canal has a correspondingly larger radius. Anteriorly, the canal terminates in a laterally crushed ampulla which connects with a small utricular recess.

Finally, it is noteworthy that although the calcified walls of the skeletal labyrinth record details of the membranous labyrinth, little is preserved of the canals for vagus and glossopharyngeal nerves.

## 4. Discussion

### 4.1. Comparative morphology

The new restoration of the *Tristychius* neurocranium (Fig. 3) builds on Dick's (1978) version (Fig. 1) and allows a better

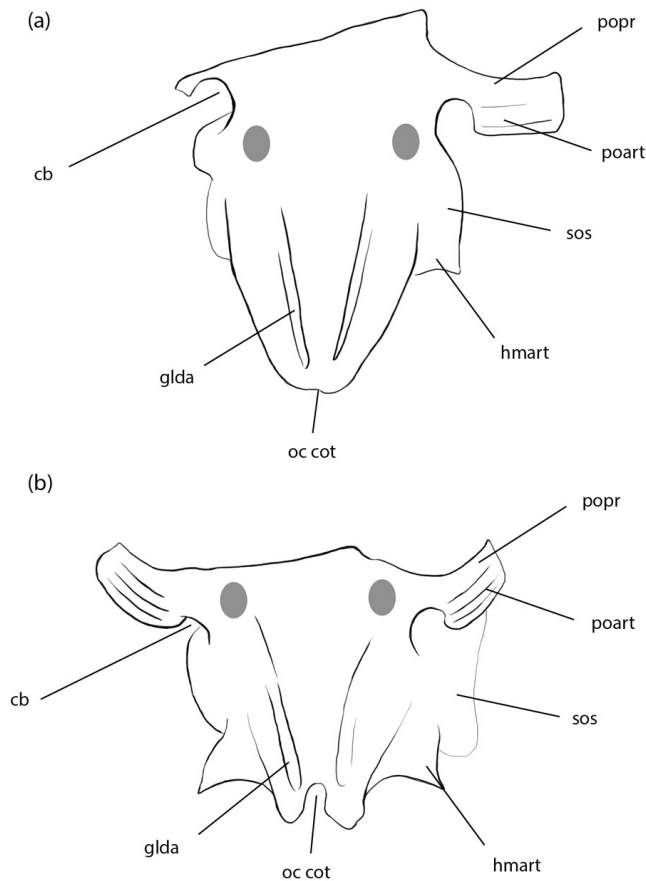


**Figure 12** Basioccipital, hypotic lamina and postorbital process positions compared in (a) *Tristychius* and (b) *Acronemus* (after Maisey 2011, text-fig. 2). Abbreviations: cb = C-bout; glda = grooves for lateral dorsal aortae; hmart = hyomandibula articulation area; oc cot = occipital cotylus; poart = postorbital articulation; popr = postorbital process; sos = supraotic shelf. Elliptical areas in grey indicate areas occupied by anterior ampulla.

assessment of its place in early chondrichthyan phylogeny. Consistent with Pradel *et al.*'s (2011) analysis of early sharks, *Tristychius* is a crown chondrichthyan because it exhibits a suite of derived conditions: a posterior tectum bridging the otic roof; closed otico-occipital and metotic fissures (in adults); an occipital arch wedged between the otic capsules; grooves rather than canals for dorsal lateral aortae in the basicranial cartilage. Further to this, *Tristychius* is a euselachian in the sense of Maisey's (2011) definition, meaning that it joins a monophyletic group including the hybodonts plus neoselachians (elasmobranchs and their immediate fossil relatives). *Tristychius* euselachian synapomorphies include a perilymphatic fenestra; a glossopharyngeal canal that was very likely floored by the hypotic lamina (although the canal itself is barely preserved, the exit of the canal suggests that an alternative arrangement would be very unlikely); a chondrified medial capsular wall; and the absence of a crus commune joining the anterior and posterior semicircular canals. In addition to these features, the newly revealed presence of a pre-ampullary section of the posterior semicircular canal extending dorsally to the perilymphatic fenestra (Fig. 11) represents a further derived characteristic that can be added to the euselachian synapomorphy list (Maisey *et al.* 2004; Coates & Gess 2007).

However, this is where the straightforward diagnosis of *Tristychius* affinities peters out. Despite the abundance of new detail, further evidence linking *Tristychius* to either of the primary euselachian lineages, the Neoselachii or the Hybodontiformes, is difficult to find. This is important because the

evolutionary split between neoselachians and hybodonts likely dates back ~340 my (Coates & Gess 2007; Maisey 2011) on the basis of the hybodont characteristics of the contemporary genus *Onychoselache* (Dick 1978; Dick & Maisey 1980; Coates & Gess 2007). However, *Tristychius* is preserved in far more detail, and more precise and accurate placement of this genus will introduce considerably more character data to phylogenetic hypotheses concerned with the elasmobranch stem lineage origin.

Pradel *et al.* (2011) joined *Tristychius* to the hybodonts on the basis of the trochlear nerve foramen situated anterior to the optic nerve foramen (Coates & Sequeira 1998; Coates & Gess 2007). But this characteristic is now absent (Figs 2d, e, 3), and the revised pattern of orbit foramina resembles the less specialised arrangements of outgroups such as *Tamiobatis vetustus* (Schaeffer 1981, fig. 19C). Lane's (2010) comparisons of *Tribodus* and *Egertonodus* identified a further series of hybodont neurocranial specialisations, but these, too, are absent in *Tristychius*. Candidate synapomorphies include the presence of a single large foramen for the combined exit of the glossopharyngeal and vagus nerves; in contrast, *Tristychius* retains separate foramina (Fig. 7c, d). In *Tribodus* and *Egertonodus*, two large openings, probably for anterior and posterior octaval nerve branches, connect the cranial cavity to the otic capsule. In *Tristychius* and neoselachians, this octaval nerve foramen is single. Anterior and posterior semicircular canals in *Egertonodus* and *Tribodus* are widely separated, but in *Tristychius*, and in crown gnathostomes in general, these canals are closely spaced. In *Egertonodus* and *Tribodus*, the anterior and posterior semicircular canals are similarly sized (radius of curvature). Once again, *Tristychius* exhibits the general gnathostome condition, in which the proportions of these canals differ.

*Tristychius* is further distanced from the base of the conventional hybodont lineage by the absence of cephalic spines, the absence of a large downturned postorbital process, and the presence (i.e., phylogenetic persistence) of a postorbital articulation for the palatoquadrate. Added to these, hybodontids and neoselachians are united (to the exclusion of *Tristychius*) by the position of the anterior ampulla between the postorbital processes (Maisey 1989, 2011; Maisey *et al.* 2004; Coates & Gess 2007).

*Tristychius* thus occupies an *incertae sedis* location outside of the main euselachian cluster. However, this solution fails to account for the hybodont-like postorbital process profile and the neurocranial features, noted in the description, that it shares with *Acronemus*. Furthermore, although the *Tristychius* postorbital process is anteroposteriorly narrow, like those of hybodonts and *Acronemus*, the process is downturned (Figs 3, 4) with an anhedral angle to the basicranium (Maisey 2011). This is markedly unlike those of xenacanth, *Tamiobatis*, *Cladodoides* and symmoriids. Anteroposterior enlargement of the process and related jugular canal changes are likely hybodont specialisations exclusive of *Tristychius*. The presence of a palatoquadrate articulation surface on the process is plesiomorphic, but a partly or completely ventral articulation surface is unusual (*cf.* Maisey's (2008) comments on Dick's (1978) reconstruction). It follows that the shared configuration of the ventral articulation surface, consisting of one or more ridges and grooves curving laterally and anteriorly, represents a likely synapomorphy linking *Acronemus* and *Tristychius* (Fig. 12).

In *Tristychius*, the articulation surface on the palatoquadrate dorsal rim (Dick 1978) consists of a transverse groove immediately anterior to the extremely reduced otic process, and presents a precise match to the ventral surface of the postorbital process. In *Acronemus*, only the lateral surface of the palatoquadrate is revealed (Rieppel 1982, text-figs 1, 2), thus no part of the articulation is visible. However, an unnamed Lower Triassic shark from Madagascar includes an extremely *Acronemus*-like

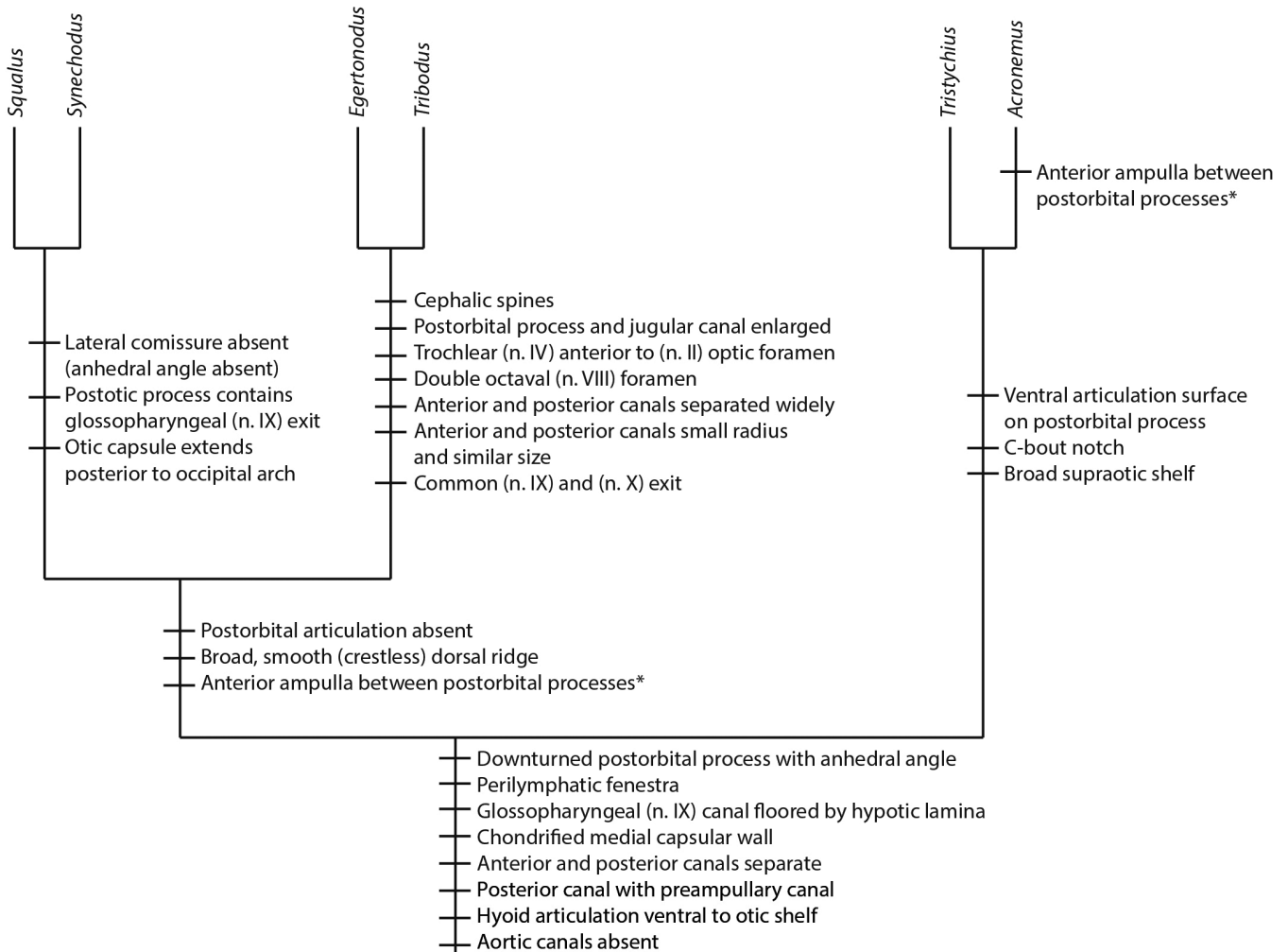


**Figure 13** Cladistic hypothesis of neurocranial character distribution among a small sample of early euselachians and the extant spiny dogfish, *Squalus*. Homoplastic character marked with asterisk. Sources of character information: *Squalus* – Schaeffer 1981, Gans & Parsons 1964, Marinelli & Strenger 1959; *Synechodus* – Maisey 1985; *Egertonodus* – Maisey 1983, Lane 2010; *Tribodus* – Lane 2010; *Acronemus* – Maisey 2011.

three-dimensionally preserved palatoquadrate, Meckel's cartilage and dentition (Thomson 1982). Significantly, this palatoquadrate, with a characteristically reduced otic process, displays a well-formed transverse and slightly anterolaterally oriented articulation surface resembling that of *Tristychius*. A *Tristychius*-style postorbital process and articulation seems also to be present in the Lower Triassic *Homalodontus* (Mutter *et al.* 2007, 2008) of British Columbia, Canada. *Homalodontus*, already compared with *Hybodus* and *Egertonodus*, is known only from dorso-laterally flattened material. But, its neurocranium, palate, lower jaw and fragmented gill skeleton in many respects resemble intermediates between outgroups such as *Tamiobatis* and the kinds of conditions now emerging in *Tristychius*.

The breadth of the otic region in *Tristychius* reflects the span of the otic capsules, rather than increased width of the main cranial cavity (Figs 4b, 10). The shape and size of the supraotic shelves relative to the rest of the preserved neurocranium is, once again, a distinctive characteristic shared with *Acronemus*. The C-bout separating the anterior limit of the otic shelf from the postorbital process is also shared with *Acronemus*. None of these features is known in hybodonts, *Tamiobatis*, xenacanth or symmoriids. Differences between *Tristychius* and *Acronemus* crania (posterior to the postorbital processes) seem to relate mostly to the extent of occipital arch intrusion between the posterior semicircular canals. A view of the ventral surfaces reinforces this interpretation (Fig. 12).

The basioccipital cartilages and hypotic laminae of *Tristychius* and *Acronemus* are more-or-less interchangeable, each with similarly divergent, deep, linear grooves for the lateral dorsal aortae. A key difference concerns the anteroposterior position of this unit (lamina plus occipital arch) relative to the otic capsules and postorbital processes. In *Tristychius*, the occipital arch and hypotic lamina are located posteriorly, but in *Acronemus* (Maisey 2011), the entire structure appears to have been shunted forwards.

Two further features of the otic region in *Tristychius* are of likely phylogenetic significance: the *Tamiobatis*-like horizontal crests on the dorsal ridge; and the sub-shelf location of the hyomandibular attachment to the otic wall. Elongate horizontal crests of the dorsal ridge are completely unknown in hybodonts, and their discovery in *Tristychius* was unexpected. Unfortunately, the dorsal surface of *Acronemus* is too poorly preserved to reveal crest presence or absence. The generally *Tamiobatis*-like (or *Orthacanthus*-like) shape of the dorsal ridge and crest in *Tristychius* suggests that this is simply a conserved plesiomorphy. If so, then the presence of a broad, smooth and crestless dorsal ridge emerges as a derived condition and possible synapomorphy of neoselachians and hybodonts, further weakening the *Tristychius*–hybodont connection.

The significance of a lateral otic shelf, and relation to possibly homologous otic shelves in modern selachians is explored by Maisey (2011) in his discussion of *Acronemus*. Here, the

similarity with modern selachian conditions is noted, alongside similarities with the shelf-like ‘postorbital process’ (Maisey 1983, 1985) of *Egertonodus* and *Synechodus*. It appears that the *Tristychius* hyoid attachment area shares characteristics with euselachians in general. Notably, none of these taxa exhibits the classic lateral otic process of early chondrichthyan crania (Schaeffer 1981) which, to a greater or lesser extent, is an extension of the posterior semicircular canal wall.

#### 4.2. Phylogenetic relationships

Cladograms of hybodont sharks started with Maisey’s (1989, fig. 35) discussion of the likely relationships of the Pennsylvanian genus *Hamiltonichthys*. In this, *Tristychius* is the sister group to all other Hybodontiformes. A modified version of this tree in Maisey *et al.* (2004, fig. 2) accommodated *Tribodus*, but *Tristychius* and its contemporary, *Onychoselache* (Dick & Maisey 1980), were excluded because of uncertainties about the accuracy of available descriptions and the seeming primitiveness of these genera. Coates & Gess (2007, text-fig. 10), as part of their revision of *Onychoselache*, re-examined these data and used a modestly expanded character set to reinstall both *Onychoselache* and *Tristychius* within the Hybodontiformes, exclusive of the Neoselachii.

In contrast to these previous hypotheses, the present cladogram (Fig. 13) is much simpler, and restricted to a handful of more anatomically disparate genera. Furthermore, the character set is concerned only with neurocranial features or other aspects of cranial skeletal anatomy connected directly to the neurocranium. The branching pattern offered here will be tested in future publications, with substantial additions of characters and taxa, and subjected to a variety of numerical analyses. For the purposes of the present discussion, this proposal offers new groups and characterisations that deserve consideration.

Here, in addition to the standard list of synapomorphies (discussed previously), the Euselachii is further supported by the following derived conditions: a postorbital process with a downturned (anhedral) angle; a hyoid articulation located on the posterior part of the otic capsule lateral wall beneath a laterally projecting shelf; and grooves rather than canals in the basicranial cartilage for the dorsal lateral aortae. This last condition depends upon outgroup choice, which in this instance is *Cladodoides* (Maisey 2005) *Tamiobatis* or *Orthacanthus* (Schaeffer 1981). If, on the other hand, these genera are replaced with fossil chimaeroids, then the presence of such grooves rather than canals for the lateral dorsal aortae becomes a synapomorphy of crown chondrichthyans.

Euselachians are divided into two clades (Fig. 13), one of which is named provisionally the Tristychiidae (acknowledging that this is a further use of the notional family coined by Moy-Thomas (1936), Dick (1978) and Ginter *et al.* (2010)). Here, the Tristychiidae includes, at minimum, *Tristychius* and *Acronemus*, and their defining synapomorphies include: a postorbital process articulation for the palatoquadrate located mostly on the ventral surface of the postorbital process; a wide and almost parallel-sided (in dorsal view) otic region; a C-bout shaped notch dividing the proximal part of the postorbital process from the anterolateral extremity of supraotic shelf.

The other primary division of the euselachian clade consists of the Neoselachii and Hybodontiformes. Synapomorphies supporting this unnamed group (informally: neoselachimorphs) include: the absence (loss) of the postorbital articulation with the palatoquadrate; a broad, smooth and crestless dorsal ridge; and the anterior projection of the otic skeletal labyrinth so that

the anterior ampulla is level with the postorbital process. This last condition either occurs independently in *Acronemus*, or it represents a euselachian synapomorphy, secondarily absent in *Tristychius*.

Hybodontiforms are defined by the presence of cephalic spines; an enlarged postorbital process; a trochlear nerve (IV) foramen anterior to the optic nerve (II) foramen; a double octaval nerve (VIII) foramen; a shared exit for glossopharyngeal (IX) and vagus (X) nerves; widely separated anterior and posterior semicircular canals; and similar radius of curvature anterior and posterior semicircular canals. Neoselachians, in turn, are defined by the loss of the lateral commissure, with the consequent absence of an anhedral angle with the basicranium; the presence of a postotic process containing the glossopharyngeal nerve (IX) exit; and an otic capsule that projects posterior to occipital arch.

There is nothing in the branching pattern and character distribution offered here that conflicts with the broader hypothesis assembled by Coates & Gess (2007). Once again, the introduction of additional genera that seem likely to be linked to the early elasmobranch radiation will provide the most effective test of this scheme. Key taxa are likely to include *Wodnika* (Schaumberg 1977; Zangerl 1981), *Hopleacanthus* (Schaumberg 1982), *Sphenacanthus* (Dick 1998), *Homalodontus* (Mutter *et al.* 2007, 2008) and a more complete description of Thomson’s (1982) unnamed hybodontid from the Triassic of Madagascar. Of these, *Sphenacanthus* (Dick 1998) is the most feasible target for further research. It already appears that the palatoquadrate otic process is reduced dorsoventrally but not anteroposteriorly, and shows no sign of articulation with the postorbital process. Thus, its upper jaw resembles that of *Onychoselache* and other hybodontids, rather than *Tristychius* and *Acronemus*. Visible parts of the *Sphenacanthus* basicranium are consistent with euselachian conditions, revealing grooves rather than canals for the lateral dorsal aortae. The new cladogram (Fig. 13), therefore, offers the possibility that *Sphenacanthus* is sister to other members of the neoselachimorph lineage. If so, and the branching pattern rests on very few character states, then the fossil fauna of the Carboniferous Oil Shales Groups of the Edinburgh region (Dick 1978, 1981, 1998; Dick & Maisey 1980; Coates & Gess 2007) captures an exemplary suite of likely early members of the early elasmobranch radiation: *Tristychius*, *Onychoselache*, *Sphenacanthus* and *Diplodoseleche*.

#### 4.3. The otic labyrinth and suggestions of palaeoecology

The various configurations of the otic labyrinth in fossil (Maisey 2001b) and Recent chondrichthyans, especially those of elasmobranchs (Evangelista *et al.* 2010; Lisney 2010), have been the focus of sporadic research interest. Aside from providing phylogenetically informative characters, skeletal signatures of labyrinth morphologies offer some indication of inner ear functional biology. Several features of modern elasmobranchs (see also Schaeffer 1981) associated with semi-directional low frequency phonoreception are clearly present in *Tristychius*: a medial capsular wall; an almost circular posterior canal; the separation of the anterior from the posterior canals (absence of a crus); a perilymphatic fenestra communicating with the parietal fossa; and a large saccular chamber. These features mark *Tristychius* as the earliest chondrichthyan yet known to show direct evidence of specialised adaptations for sound detection. In terms of the conjectured outline of elasmobranch phylogeny (Fig. 13), the acoustic adaptations of the Euselachii could reasonably be described the most characteristic, unifying feature of the clade (similarly, the neoselachimorphs might be

summarised as 'loose-jawed', given the loss of a skeletal articulation between the palate and postorbital process). This inference about the general biology of euselachians begs the question of what they were listening to. Unlike the Chondrichthyes, adaptations for phonoreception in Osteichthyes are linked to vocalisation, and osteichthyan vocalisation is sufficiently widespread, taxonomically, to suggest that vocal-acoustic mechanisms and behaviours are likely ancestral for the entire clade (Bass & Chagnaud 2012). Perhaps these early euselachians were paying attention to noises emitted by osteichthyans, as both likely predators and prey.

The inner ear of *Tristychius* is further distinguished by the broad sweep of the external canal (Fig. 10). Young (1981), noted by Maisey (2001b), associated large external (horizontal) canals (radius of canal curvature) with fishes with slow turning speeds, and vice-versa for rapid swimmers (and canals with a narrow internal radius). However, recent studies challenge the utility of canal radii measurements as accurate predictors of head movement, orientation, manoeuvrability and swimming behaviour (Evangelista *et al.* 2010). Nevertheless, of the various elasmobranch labyrinths surveyed by Evangelista *et al.* (2010), those with almost comparably large external canals relative to anterior and posterior canals, include *Carcharhinus leucas* (bull shark) and *Orectolobus maculatus* (wobbegong). Notably, anadromous bull sharks frequently enter and forage in shallow, non-marine waters, and wobbegongs are mostly benthic. Dick (1981, 1998) has repeatedly pointed out that *Tristychius* was very likely the normal inhabitant of a large fresh or brackish water lagoon. There is, at least, some consistency here, in terms of inferred swimming habits.

Last of all, the laterally compressed saccular chamber of NMS 1972.27.481D (Fig. 11c, d) is damaged: its fragmented walls are driven inwards around a near-conical depression, and a matching, although less well preserved, depression punctures the opposite side of the specimen. It appears that the lateral compression of this particular braincase resulted from a crushing bite. Furthermore, unlike dorsoventrally compressed specimens such as NMS 1974.23.6 and NMS 1974.23.30A & B, which are preserved in articulation with their visceral arches, the jaws, hyoid arch and gill skeleton of NMS 1972.27.481D are present but dismembered. Of the fishes recorded from the Wardie fauna (Dineley & Metcalf 1999), only one is known to have had teeth of sufficient size and spacing to inflict this damage, the rhizodont *Rhizodus hibberti*.

## 5. Acknowledgements

This project could not have been undertaken and completed without the dedication, talent and genius of Stan Wood. For access to specimens, we thank N. Fraser and S. Walsh of the National Museums of Scotland. Isaac Krone assisted with the rendering of CT scans. We thank J. R. F. Dick for discussion of the original collection and description of Stan Wood's material; M. Taylor for insight concerning C. W. Peach; and Andrew Bass for discussion of fish vocal-acoustic systems. Z. Johanson and M. Brazeau are thanked for insightful reviews of the manuscript. This project and, in particular, the CT scanning of specimens, was supported by National Science Foundation grants DEB-0917922 and DEB-1541491.

## 6. References

- Agassiz, L. 1837 *Recherches sur les poissons fossils* Vol. 3. Neuchâtel, Switzerland: Petitpierre.
- Bass, A. H. & Chagnaud, B. P. 2012. Shared developmental and evolutionary origins for neural basis of vocal-acoustic and pectoral-gestural signaling. *Proceedings of the National Academy of Science* **109**, 10677–84.
- Clarkson, E. N. K. 1986. Granton and Wardie shore. In McAdam A. D. & Clarkson, E. N. K. (eds) *Lothian Geology: an excursion guide*, 76–80. Edinburgh: Scottish Academic Press. 221 pp.
- Coates, M. I., Gess, R. W., Flynn, J. A., Criswell, K. E. & Tietjen, K. 2017. A symmoriiform chondrichthyan braincase and the origin of chimaeroid fishes. *Nature* **541**, 208–11.
- Coates, M. I. & Gess, R. W. 2007. A new reconstruction of *Onychoselache traquairi*, comments on early chondrichthyan pectoral girdles and hybodontiform phylogeny. *Palaeontology* **50**, 1421–46.
- Coates, M. I. & Sequeira, S. E. K. 1998. The braincase of a primitive shark. *Transactions of the Royal Society of Edinburgh: Earth Sciences* **89**, 63–85.
- Daniel, J. F. 1922. *The Elasmobranch Fishes*. Berkeley: University of California Press. 332 pp.
- Davis, S. P., Finarelli, J. A. & Coates, M. I. 2012. *Acanthodes* reveals shark-like conditions in last common ancestor of modern jawed vertebrates. *Nature* **486**, 247–50.
- de Beer, G. R. 1937. *The Development of the Vertebrate Skull*. Chicago: University of Chicago Press. xxiii + 552 pp.
- Dick, J. R. F. 1978. On the Carboniferous shark *Tristychius arcuatus* Agassiz from Scotland. *Transactions of the Royal Society of Edinburgh* **70**, 63–109.
- Dick, J. R. F. 1981. *Diplodoseleche woodi* gen. et sp. nov., and early Carboniferous shark from the Midland Valley of Scotland. *Transactions of the Royal Society of Edinburgh: Earth Sciences* **72**, 99–113.
- Dick, J. R. F. 1998. *Sphenacanthus*, a Palaeozoic freshwater shark. *Zoological Journal of the Linnean Society* **122**, 9–25.
- Dick, J. R. F. & Maisey, J. G. 1980. The Scottish Lower Carboniferous shark *Onychoselache traquairi*. *Palaeontology* **23**, 363–74.
- Dineley, D. L. & Metcalf, S. J. 1999. Fossil fishes of Great Britain. *Geological Conservation Review Series* **16**. Peterborough: Joint Nature Conservation Committee. 675 pp.
- Dupret, V., Sanchez, S., Goujet, D., Tafforeau, P. & Ahlberg, P. 2014. A primitive placoderm sheds light on the origin of the jawed vertebrate face. *Nature* **507**, 500–03.
- Evangelista, C., Mills, M., Siebeck, U. E. & Collin, S. P. 2010. A comparison of the external morphology of the membranous inner ear in elasmobranchs. *Journal of Morphology* **271**, 483–95.
- Gans, C. & Parsons, T. S. 1964. *A Photographic Atlas of Shark Anatomy: The Gross Morphology of Squalus Acanthias*. New York: Academic Press. 112 pp.
- Gardiner, B. G. 1984. The relationships of the palaeoniscid fishes, a review based on new specimens of *Mimia* and *Moythomasia* from the Upper Devonian of Western Australia. *Bulletin of the British Museum (Natural History) Geology* **37**, 173–428.
- Ginter, M., Hampe, O. & Duffin, C. 2010. Chondrichthyes 3D, Paleozoic Elasmobranchii: Teeth. In Schultze, H.-P. (ed.) *Handbook of Paleoichthyology*. München: Verlag Dr. Friedrich Pfeil. 512 pp.
- Hay, O. P. 1902. Bibliography and catalogue of the fossil vertebrates of North America. *Bulletin of the United States Geological Survey* **179**, 1–868.
- Huxley, T. H. 1880. *A manual of the vertebrated animals*. New York: D. Appleton. viii + 698 pp.
- Janvier, P. 1996. *Early Vertebrates. Oxford Monographs on Geology and Geophysics* **33**. Oxford: Clarendon Press. 408 pp.
- Lane, J. A. 2010. Morphology of the braincase in the Cretaceous hybodont shark *Tribodus limnae* (Chondrichthyes: Elasmobranchii), based on CT scanning. *American Museum Novitates* **2758**, 1–70.
- Lisney, T. J. 2010. A review of the sensory biology of chimaeroid fishes (Chondrichthyes: Holocephali). *Reviews in Fish Biology and Fisheries* **20**, 571–90.
- Long, J. A., Mark-Kurik, E., Johanson, Z., Lee, M. S. Y., Young, G. C., Min, Z., Ahlberg, P. E., Newman, M., Jones, R., den Blauwen, J., Choo, B. & Trinjastic, K. 2015. Copulation in antiarch placoderms and the origin of gnathostome fertilization. *Nature* **517**, 197–99.
- Maisey, J. G. 1983. Cranial anatomy of *Hybodus basanus* Egerton from the Lower Cretaceous of England. *American Museum Novitates* **2758**, 1–64.
- Maisey, J. G. 1985. Cranial anatomy of the fossil elasmobranch *Synechodus dubrisiensis*. *American Museum Novitates* **2857**, 1–16.
- Maisey, J. G. 1987. Cranial anatomy of the Lower Jurassic shark *Hybodus reticulatus* (Chondrichthyes; Elasmobranchii), with comments on hybodontid systematics. *American Museum Novitates* **2878**, 1–39.
- Maisey, J. G. 1989. *Hamiltonichthys mapesi* g. & sp. nov. (Chondrichthyes; Elasmobranchii), from the Upper Pennsylvanian of Kansas. *American Museum Novitates* **2931**, 1–42.

Agassiz, L. 1837 *Recherches sur les poissons fossils* Vol. 3. Neuchâtel, Switzerland: Petitpierre.

Bass, A. H. & Chagnaud, B. P. 2012. Shared developmental and evolutionary origins for neural basis of vocal-acoustic and pectoral-



- Maisey, J. G. 2001a. A primitive chondrichthyan braincase from the Middle Devonian of Bolivia. In Ahlberg, P. E. (ed.) *Major Events in Early Vertebrate Evolution*, 263–88. London: Taylor and Francis. xiv + 418 pp.
- Maisey, J. G. 2001b. Remarks on the inner ear of elasmobranchs and its interpretation from skeletal labyrinth morphology. *Journal of Morphology* **250**, 236–64.
- Maisey, J. G. 2004. Endocranial morphology in fossil and recent chondrichthyans. In Arratia, G., Wilson, M. V. H. & Cloutier, R. (eds) *Recent Advances in the Origin and Early Radiation of Vertebrates*, 139–70. München: Verlag Dr. Friedrich Pfiel. 703 pp.
- Maisey, J. G. 2005. Braincase of the Upper Devonian shark *Cladodoides wildungensis* (Chondrichthyes, Elasmobranchii), with observations on the braincase in early chondrichthyans. *Bulletin of the American Museum of Natural History* **288**, 1–103.
- Maisey, J. G. 2007. The braincase in Paleozoic symmoriiform and cladoselachian sharks. *Bulletin of the American Museum of Natural History* **307**, 1–122.
- Maisey, J. G. 2008. The postorbital palatoquadrate articulation in elasmobranchs. *Journal of Morphology* **269**, 1022–40.
- Maisey, J. G. 2011. The braincase of the Middle Triassic shark *Acronemus tuberculatus* (Bassani, 1886). *Palaeontology* **54**, 417–28.
- Maisey, J. G., Naylor, G. J. P. & Ward, D. J. 2004. Mesozoic elasmobranchs, neoselachian phylogeny and the rise of modern elasmobranch diversity. In Arratia, G. & Tintori, A. (eds) *Mesozoic Fishes 3 – Systematics, Palaeoenvironments and Biodiversity*, 17–56. München: Verlag Dr. Friedrich Pfiel. 649 pp.
- Marinelli, W. & Strenger, A. 1959. *Vergleichende Anatomie und Morphologie der Wirbeltiere*. III. 174–308. Wien: Franz Deuticke.
- Mitchell, G. H. & Mykura, W. 1962. *The Geology of the Neighbourhood of Edinburgh* (3rd edn). *Memoirs of the Geological Survey of Great Britain*. Edinburgh: HMSO. 405 pp.
- Moy-Thomas, J. A. 1936. On the structure and affinities of the fossil elasmobranch fishes from the Lower Carboniferous rocks of Glencartholm, Eskdale. *Proceedings of the Zoological Society of London* **1936**, 761–88.
- Mutter, R. J., de Blanger, K., & Neuman, A. G. 2007. Elasmobranchs from the Lower Triassic Sulphur Mountain Formation near Wapiti Lake (BC, Canada). *Zoological Journal of the Linnean Society* **149**, 309–37.
- Mutter, R. J., Neuman, A. G. & de Blanger, K. 2008. *Homalodontus* nom. nov. a replacement for *Wapitiodus* Mutter, de Blanger and Neuman 2007 (Homalodontidae nom. nov., ?Hybodontoidae), preoccupied by *Wapitiodus* Orchard, 2005. *Zoological Journal of the Linnean Society* **154**, 419–20.
- Peach, B. N., Gunn W., Clough C. T., Hinxman, L. W., Grant Wilson, J. S., Crampton, C. B., Maufe, H. B. & Bailey, E. B. 1910. *The Geology of the Neighbourhood of Edinburgh* (2nd edn). *Memoirs of the Geological Survey of Scotland*. HMSO, Edinburgh, 405 pp.
- Pradel, A. 2010. Skull and brain anatomy of Late Carboniferous Sibirhinchidae (Chondrichthyes, Iniopterygia) from Kansas and Oklahoma (USA). *Geodiversitas* **32**, 595–661.
- Pradel, A., Tafforeau, P., Maisey, J. G. & Janvier, P. 2011. A new Paleozoic Symmoriiformes (Chondrichthyes) from the Late Carboniferous of Kansas (USA) and Cladistic Analysis of Early Chondrichthyans. *PLoS ONE* **6**: e24938 doi:10.1371/journal.pone.0024938.
- Pradel, A., Maisey, J. G., Tafforeau, P., Mapes, R. H. & Mallatt, J. 2014. A Palaeozoic shark with osteichthyan-like branchial arches. *Nature* **509**, 608–11.
- Rieppel, O. 1982. A new genus of shark from the Middle Triassic of Monte San Giorgio, Switzerland. *Palaeontology* **25**, 399–412.
- Schaeffer, B. 1981. The xenacanth shark neurocranium, with comments on elasmobranch monophyly. *Bulletin of the American Museum of Natural History* **169**, 1–66.
- Schaumburg, G. 1977. Der Richelsdorfer Kupferschiefer und seine Fossilien III. Die tierischen Fossilien des Kupferschiefers, 2. Vertebraten. *Aufschluss* **28**, 297–351.
- Schaumburg, G. 1982. *Hopleacanthus richelsdorfi* n. g. n. sp., ein Euselachier aus dem permischen Kupferschiefer von Hessen (W-Deutschland). *Paläontologisches Zeitschrift* **56**, 235–57.
- Taylor, M. A. & Anderson, L. I. 2015. Additional Information on Charles W. Peach (1800–1886). *The Geological Curator* **10**, 159–80.
- Thomson, K. S. 1982. An Early Triassic Hybodont Shark from Northern Madagascar. *Postilla* **186**, 1–16.
- Traquair, R. H. 1903. On the distribution of fossil fish remains in the Carboniferous rocks of the Edinburgh district. *Transactions of the Royal Society of Edinburgh* **40**, 687–707.
- Waterston, 1962. Excursion D – Wardie and Granton shore. In Mitchel, G. H., Walton, K. & Grant, D. (eds) *Edinburgh Geology: An Excursion Guide*, 20–22. Edinburgh: Oliver & Boyd. xv + 222 pp.
- Wood, S. P. 1975. Recent discoveries of Carboniferous fishes in Edinburgh. *Scottish Journal of Geology* **11**, 251–58.
- Young, J. Z. 1981. *The life of vertebrates*. 3rd Ed. Oxford: Clarendon Press. 645 pp.
- Zangerl, R. 1981. Chondrichthyes I: Paleozoic Elasmobranchii. In Schultze, H.-P. (ed.) *Handbook of Paleichthyology*. Stuttgart: Gustav Fischer Verlag. 115 pp.

---

MS received 18 November 2016. Accepted for publication 2 May 2017.